Appl. Phys. A 74 [Suppl.], S937–S939 (2002) / Digital Object Identifier (DOI) 10.1007/s003390201684

Applied Physics A
Materials
Science & Processing

Multiple small-angle neutron scattering studies of anisotropic materials

Andrew J. Allen[1,*], **Norman F. Berk**[1], **Jan Ilavsky**[1,2], **Gabrielle G. Long**[1]

[1] NIST, Gaithersburg, MD 20899, USA
[2] University of Maryland, College Park, MD 20742, USA

Received: 16 July 2001/Accepted: 13 November 2001 –

Abstract. Building on previous work that considered spherical scatterers and randomly oriented spheroidal scatterers, we describe a multiple small-angle neutron scattering (MSANS) analysis for nonrandomly oriented spheroids. We illustrate this with studies of the multi-component void morphologies found in plasma-spray thermal barrier coatings.

PACS: 61.12.Ex; 61.43.Gt; 61.72.Qq

The small-angle neutron scattering (SANS) associated with the concentrated, micrometer-scale voids found in materials of technological interest (porous ceramics, coatings, etc.) frequently is dominated by multiple scattering. Sizes and volume-fractions usually obtained by SANS cannot then be retrieved merely by correcting data. A multiple-SANS (MSANS) analysis is needed to recover this information directly from the measurements. Previously, a MSANS formalism to do this was developed for an ensemble of spherical scatterers [1] that has been validated in ceramic sintering studies [2]. More recently, it has been extended to treat a random distribution of nonspherical scatterers such as the coin-shaped pores produced during the sintering of certain silica gels [3]. The MSANS formalism implicitly assumes the microstructure and scattering to be axially symmetric about the incident beam direction, and it cannot directly interrogate general anisotropic microstructures. However, circularly averaged MSANS data can be analyzed, and then the anisotropy examined independently. Many anisotropic microstructures of interest, e.g., thermal barrier coatings (TBC's), contain several void systems, which often are axially symmetric about the normal to the susbstrate. Furthermore, the components can be distinguished by Porod scattering, which amplifies the anisotropy [4]. Several parameters are needed to relate the void components to each other, and the MSANS formalism thus must be constrained to model only those microstructures consistent with the measured total porosity and void specific (Porod) surface area.

*Corresponding author.
(Fax: +1-301/975-5334, E-mail: andrew.allen@nist.gov)

In this paper we present the new MSANS formalism for anisotropic microstructures and illustrate its application to one TBC system. Detailed application of the technique can be found in [5].

1 Theoretical treatment

Previously, it was shown how the mean radius, R_0, of a coarse, concentrated ensemble of spherical scatterers with known volume fraction, Φ_T, is obtainable from the variation of MSANS beam broadening with incident neutron wavelength, λ [1]. Refraction and diffraction are included in deriving the multiple-scattered beam Q-profile, $W(QR_0, \tau_s)$, after passing through a sample thickness, τ_s, where $Q = (4\pi/\lambda)\sin\theta$ is the magnitude of the scattering vector, and 2θ is the scattering angle. Theoretically, the "radius of curvature", r_c, of the multiple-scattered beam profile (in units of Q) is given by

$$r_c = \lim_{Q\to 0}\left[\frac{W''(QR_0, \tau_s)}{W(QR_0, \tau_s)}\right]^{-\frac{1}{2}} , \tag{1}$$

where $''$ indicates the second derivative with respect to Q. For measurement purposes, r_c is numerically equal to the standard deviation (in Q) of a Gaussian shape profile fitted to the MSANS-broadened beam profile in the vicinity of $Q = 0$. This does not mean that the beam profile is a convolution of single-scatter Gaussians using the Central Limit Theorem (CLT). The CLT does not apply to MSANS, in fact, because of Q^{-4} Porod scattering at large Q [1, 3]. The MSANS formalism uses first-principles arguments to derive $W(QR_0, \tau_s)$ by considering in- and out-scatter terms as the neutron beam passes through the sample to give

$$W(QR_0, \tau_s) = \frac{k_0^2 R_0^2}{2\pi}\int_0^\infty J_0(QR_0\zeta)e^{-\bar{z}[1-q(\zeta)]}\zeta\, d\zeta , \tag{2}$$

where $k(= 2\pi/\lambda)$ is the magnitude of the incident and scattered wavevector, $\bar{z}$ is the average number of multiple scatters

within the sample, J_0 is the Bessel function of zero order, ζ is a dimensionless integration variable, and $q(\zeta)$ is a real-space function discussed below.

While originally derived for spheres, it was recognized [3] that the formalism can be applied to a random distribution of nonspherical scatterers, since the scattering remains axially symmetric about the incident beam. In fact with axial symmetry, not even a random orientation distribution is necessary. The $q(\zeta)$ can be expressed in terms of any axially symmetric average of the single-scatter cross-section, $\sigma(\boldsymbol{Q}, \nu_0)$, and the corresponding total cross-section, σ_T, such that:

$$q(\zeta)=\frac{2\pi}{k^2}\,\langle\sigma_T\rangle_\Omega\int_0^\infty J_0(QR_0\zeta)\,\langle\sigma(\boldsymbol{Q},\nu_0)\rangle_\Omega\,Q\mathrm{d}Q\,. \tag{3}$$

The neutron phase shift parameter, $\nu_0 = 2R_0|\Delta\rho|\lambda$, signals that both refraction and diffraction are significant for large scattering features. The orientational averages, $\langle\cdots\rangle_\Omega$, are over the scatterer orientation distribution for a fixed sample orientation. These can be determined readily for axial symmetry about the incident beam direction, which is attained by circularly averaging the MSANS beam-broadening data. Any actual MSANS anisotropy observed for a given sample orientation is treated separately. For nonrandom scatterer orientation distributions, $\langle\sigma(\boldsymbol{Q},\nu_0)\rangle_\Omega$ and $\langle\sigma_T\rangle_\Omega$ depend on the sample orientation, as does $\bar{z}$, which equals $n_T\,\langle\sigma_T\rangle_\Omega\,\tau_s$, where n_T is the total number density of scatterers. To derive the functional form for the orientationally averaged single-scatter cross-sections assumptions must be made concerning the shape and orientation distribution of the scatterers. One versatile model shape for the scatterers is an oblate or prolate spheroid of aspect ratio, β, and three orthogonal radii, R_0, R_0, and βR_0. At a given angle, η, of the βR_0 spheroid axis with respect to the direction of $\boldsymbol{Q}$ it can be shown [3] that $\sigma_{\beta,\chi}(\boldsymbol{Q},\nu_0)=\left|f_{\beta,\chi}(\boldsymbol{Q},\nu_0)\right|^2$, where

$$f_{\beta,\chi}(\boldsymbol{Q},\nu_0)=\mathrm{i}kR_0^2K(\beta,\chi)\times \int_0^1 J_0(QR_0K(\beta,\chi)\xi)\left[1-\mathrm{e}^{\mathrm{i}\beta\nu_0\sqrt{1-\xi^2}/K(\beta,\chi)}\right]\xi\mathrm{d}\xi\,, \tag{4}$$

and $K(\beta,\chi)=\left[1+(\beta^2-1)\chi^2\right]^{\frac{1}{2}}$; $\chi=\cos\eta$, and ξ is a dimensionless integration variable, different from ζ in (3). Furthermore, $\sigma_{\chi,T}=\pi R_0^2A_\chi(\beta,\nu_0)$, with

$$A_\chi(\beta,\nu_0)=K(\beta,\chi)\left[2+\frac{4}{c^2}\,(1-\cos c-c\sin c)\right] \tag{5}$$

and $c=\beta\nu_0/K(\beta,\chi)$.

For a random orientation distribution, the orientational averages can be determined from the integrals, $\langle\sigma(\boldsymbol{Q},\nu_0)\rangle_\Omega=\int\sigma_{\beta,\chi}(\boldsymbol{Q},\nu_0)\mathrm{d}\chi$ and $\langle\sigma_T\rangle_\Omega=\int\sigma_{\chi,T}\mathrm{d}\chi$ over the interval $\chi=(0,1)$. For a nonrandom distribution, axially symmetric about the incident beam, these integrals can be weighted over different parts of the χ range by assuming that the direction of $\boldsymbol{Q}$ lies approximately in the plane perpendicular to the incident beam. With the incident beam parallel to the symmetry axis, this orientational weighting directly reflects the axially symmetric microstructure. For an orthogonal sample orientation, a coordinate transformation is needed to give the orientation distribution with respect to the new incident beam direction. This distribution must then be circularly averaged to give the axially symmetric distribution for the circularly averaged MSANS. Typically, the anisotropic MSANS data are averaged in 15°-wide sectors around the incident beam, and a simple scatterer orientation distribution is expressed in terms of the probability of finding the βR_0 spheroid axis, in each of the ranges 0°–30°, 30°–60°, and 60°–90° with respect to the axis of symmetry. For given Φ_T and n_T, it is possible to follow the equations back from (5) through (1) to model the MSANS r_c versus λ data. As with a random scatterer orientation, determination of $q(\zeta)$ from (3) is simplified because the integral need only be taken over the range $0<Q<4\pi/\lambda$, and in determining $W(QR_0,\tau_s)$ from (2), the integrand is nonzero only for $0<\zeta<2$ when $\beta<1$, and for $0<\zeta<2\beta$ when $\beta>1$ [3]. In modelling the MSANS anisotropy observed with the incident beam orthogonal to the symmetry axis, the anisotropic variation is assumed to follow that of the single-scatter cross-section, averaged over the orientation distribution. At least in the diffraction limit of $\nu_0<<1$, this variation is proportional to $[R_0K(\beta,\chi)]^{-1}$ for a fixed spheroid orientation.

Multiple void components must now be accommodated into the formalism. In plasma-spray TBC's, the three main void types are intrasplat cracks, denoted C and mainly perpendicular to the substrate, interlamellar pores, denoted P and mainly parallel to the substrate, and globular pores, denoted G. To model the MSANS data, each of the C and P void systems are assumed to comprise networks of oblate spheroidal elements with aspect ratios, β_c and β_P, with mean oblate radii, R_{0C} and R_{0P}, and with different orientation distributions with respect to the axis of symmetry. The globular pores are assumed to be spheres of mean radius, R_{0G}. The porosities, Φ_c, Φ_P and Φ_G, number densities, n_c, n_P and n_G, and many of the previously-defined parameters can be divided into contributions from the three void components. However, a key point is that inspection of (2) and (3), if expressed in terms of R_{0C}, shows that

$$\bar{z}q(\zeta)=\bar{z}_cq_c(\zeta)+\bar{z}_Pq_P(\zeta_P)+\bar{z}_Gq_G(\zeta_G)\,, \tag{6}$$

where $\zeta_P=\zeta R_{0C}/R_{0P}$, $\bar{z}_c=n_c\sigma_c\tau_s$, etc. Thus, the orientationally-averaged scattering from each void component can be computed separately using (3)–(5) and then combined in (2) using the result of (6) to give the predicted MSANS r_c value defined by (1). For analysis of the MSANS anisotropy, the component anisotropies are weighted both by $\bar{z}$ and R_0^{-1} to account for the relative widths of the single-scatter functions.

The aspect ratios of the spheroidal elements are set to $\beta_c=1/10$ and $\beta_P=1/5$. Other model parameters must be adjusted empirically to satisfy the constraints for MSANS beam broadening and anisotropy, for Φ_T, and for the total void specific (Porod) surface area, S_T, (with the component surface areas calculated from standard expressions for a spheroid [4]). For plasma-spray deposits, typically $R_{0P}/R_{0C}\approx1$ and R_{0G}/R_{0C} falls in the range $(1.3-1.8)$. The only free parameter left is R_{0C}. Fitting is insensitive to the spheroid assumptions for the C and P void systems because their contributions to the MSANS broadening are dominated by the short (βR_0) dimensions. The mean open-

ing dimension, $\langle \text{O.D.} \rangle = 4\beta R_0/3$, in each case, is the one of interest.

2 Experimental

We demonstrate the use of the new MSANS formalism in characterizing the void components in a yttria-stabilized zirconia (8%Y_2O_3 by mass) plasma-sprayed ceramic deposit, prepared from a spheroidized powder feedstock. Free standing deposits were studied in the as-sprayed state, and annealed at 1100 °C, 1200 °C, 1300 °C and 1400 °C for 1 h. Full details are given in [5].

All SANS and MSANS measurements were performed at the 8 m SANS instrument [6] at the NIST Center for Neutron Research. The anisotropic Porod scattering was measured at $\lambda = 8$ Å, with the incident beam perpendicular to the spray direction (symmetry axis). The MSANS beam broadening was measured at wavelengths of 10 Å, 12 Å, 14 Å, 16 Å, and 18 Å, $\Delta\lambda/\lambda = 15\%$, with the incident beam both perpendicular and parallel to the spray direction. The Porod scattering and MSANS anisotropies were determined by sector-averaging, as described above.

3 Results and discussion

With the above MSANS methods, the component porosities and surfaces areas, $\langle \text{O.D.} \rangle' s$ for the C and P void systems, their orientation probabilities, and the mean globular pore diameter, $2R_G$, were measured as a function of annealing. Estimated fractional standard deviations were $\pm 10\%$ for the component porosities, and $\pm 5\%$ for the other parameters. Figure 1 presents the component porosities versus sintered density. As annealing progresses the analysis predicts a loss of cracks and interlamellar pores through sintering as annealing progresses, and a corresponding increase in globular porosity.

This picture is qualitatively confirmed by SEM studies but it is SANS and MSANS that quantify the changes and link these to properties [5]. Such changes in the anisotropic void microstructures can have profound implications for the TBC properties.

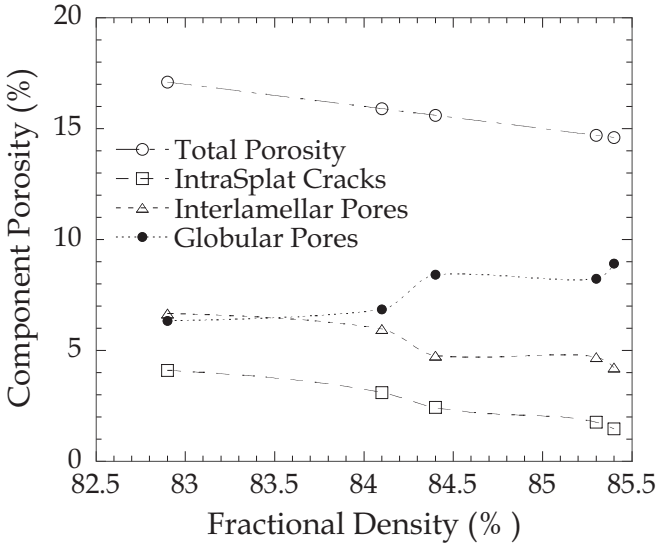

Fig. 1. MSANS-derived component porosities versus density for as-sprayed YSZ deposit (lowest density) and after annealing for 1 h at 1100 °C, 1200 °C, 1300 °C and 1400 °C (highest density). *Lines* are guides to the eye.

4 Conclusion

We have presented a MSANS formalism applicable to anisotropic multi-component microstructures. We have illustrated its application in the characterization of plasma-sprayed thermal barrier coatings.

References

1. N.F. Berk, K.A. Hardman-Rhyne: J. Appl. Cryst. **18**, 467 (1985) and **21**, 645 (1988)
2. G.G. Long, S. Krueger, A.J. Allen: J. Neutron Res. **7**, 195 (1999)
3. A.J. Allen, N.F. Berk: J. Appl. Cryst. **27**, 878 (1994)
4. J. Ilavsky, A.J. Allen, G.G. Long, S. Krueger, C.C. Berndt, H. Herman: J. Am. Ceram. Soc. **80**, 733 (1997)
5. A.J. Allen, J. Ilavsky, G.G. Long, J.S. Wallace, C.C. Berndt, H. Herman: Acta Mater. **49**, 1661 (2001)
6. C.J. Glinka, J.M. Rowe, J.G. LaRock: J. Appl. Cryst. **19**, 427 (1985)